Journal Pre-proof

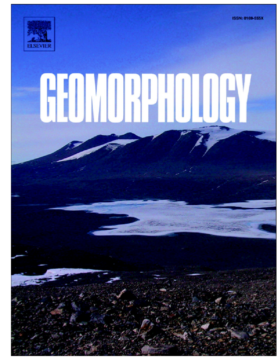

Does anthropogenic morphogenesis contribute to geomorphodiversity in urban environments?

Martina Burnelli, Alessia Pica, Maurizio Del Monte, Michele Delchiaro, Laura Melelli, Francesca Reame, Francesca Vergari, Massimiliano Alvioli

PII: S0169-555X(24)00534-8

DOI: https://doi.org/10.1016/j.geomorph.2024.109582

Reference: GEOMOR 109582

To appear in: *Geomorphology*

Received date: 5 July 2024

Revised date: 13 December 2024

Accepted date: 14 December 2024

Please cite this article as: M. Burnelli, A. Pica, M. Del Monte, et al., Does anthropogenic morphogenesis contribute to geomorphodiversity in urban environments?, *Geomorphology* (2024), https://doi.org/10.1016/j.geomorph.2024.109582

Does anthropogenic morphogenesis contribute to geomorphodiversity in urban environments?

Martina Burnelli[1,2], Alessia Pica[3]*, Maurizio Del Monte[3], Michele Delchiaro[3], Laura Melelli[1], Francesca Reame[3], Francesca Vergari[3], Massimiliano Alvioli[2]

[1] Department of Physics and Geology, University of Perugia, Piazza Università 1, 06123, Perugia, Italy

[2] Istituto di Ricerca per la Protezione Idrogeologica, Consiglio Nazionale delle Ricerche, via Madonna Alta 126, I-06128, Perugia, Italy

[3] Sapienza University of Rome, Earth Sciences p.zzle A. Moro 5, 00185 Rome, Italy

*Correspondence: alessia.pica@uniroma1.it

Abstract

Urban geomorphology studies the landscape in cities, and changes induced by human activities to the natural landscape. Cities have different geological-geomorphological substrates, and humans as "geomorphic agents" have been operating within them in different times since the Paleolithic, threatening the Earth-surface heterogeneity and ecological sustainability, especially in urban areas. Urban geomorphology helps understanding natural and historical landscape evolution, changes to natural morphologies, and the effects of the development of cities on natural geomorphological processes. Quantitative geomorphodiversity describes the variety of landforms and morphological processes characterizing the landscape. Geomorphodiversity maps can be prepared using heterogeneous spatial data, at different geographical scales. Here, we adopt the land surface diversity index of Italy, which approximates field-based geomorphological maps. One relevant example of the latter, in Italy, is the geomorphological survey carried out in Rome, which integrates field surveys, historical maps, aerial photographs, archaeological and geomorphological literature. In this work, we compare the land surface diversity index, obtained with a simple and objective approach, with comprehensive geomorphological maps of locations describing the rural-urban gradient within the Rome urban area. We aim at understanding the representativeness of the geomorphodiversity index at the local scale, and its advantages and limitations, in urban areas. We describe a simple approach to compare the geomorphodiversity index and the geomorphological dataset. The method pins down to a common ground the five diversity classes, in the raster index, and the number of landforms mapped in the field, in the geomorphological map. Most notably, the latter distinguishes natural and anthropogenic landforms, allowing us a different assessment for these substantially different geomorphological elements. Results highlight that both natural and anthropogenic processes contribute to geomorphodiversity in urban environment, and in areas having different urbanization level. They are relevant to understand the anthropogenic morphogenesis impact on geomorphodiversity in urban environment.

Keywords

Geomorphodiversity, Geomorphological mapping, Landscape classification, Urban environment, Anthropogenic erosion-accumulation

Highlights

- Anthropogenic morphogenesis modifies natural landscape in urban environments
- Locally scaled-down land surface diversity index matches real-world geomorphology
- Anthropogenic landforms contribute to geomorphodiversity as much as natural ones

Table of contents

1 Introduction

The Earth is experiencing the most populated period of its history, with urban areas increasing worldwide. Future projections report that 70% of humans will live in cities by 2050 (United Nations, 2012). Uncontrolled expansion of built-up areas has a huge demand for land and a large impact on natural systems surrounding urban areas.

Urban ecology recently emerged as a discipline (Sabogal, 2021), which discusses cities either as integrated ecosystems (Rebele, 1994) or as ecosystems themselves (Grenier et al., 2020). To analyze ecological sustainability, urban ecology studies are paying increasing attention to the anthropic impact on urban ecosystem processes and components. This led to the development of Essential Variables (Bojinski et al., 2014), and Essential Geodiversity Variables (EGVs; Scrhodt et al., 2019). EGVs aim to “quantify and monitor heterogeneity of Earth-surface and subsurface abiotic features, including geology, geomorphology, hydrology and pedology” (Schrodt et al., 2024).

In this framework, geodiversity assessment in urban areas may represent an indicator of human impact on the environment, for what concerns abiotic components. Few geodiversity studies investigate urban environment, mainly focused on ecosystem services provided by geodiversity and impacted by human activity (da Silva and do Nascimento, 2020; Reverte et al., 2020; Balaguer et al., 2022, 2023), geodiversity elements inventory and assessment for geotourism (Pica et al., 2016; Kubalíková et al., 2017; Pica et al., 2017; Kubalíková et al., 2018; Pica et al., 2018; Kubalíková et al., 2019; Mucivuna et al., 2019; Moradipour et al., 2020; Kubalíková et al., 2021; Wolniewicz, 2022) and urbanization planning and management (Ilić et al., 2016; Santos et al., 2017). Geomorphology is less investigated than other geodiversity component (Hubert et al., 2019; Burnelli et al., 2024), in fact quantifying the impact of human activities on geomorphological processes is poorly represented in the scientific literature, and this work goes the direction of filling this gap.

The focus of urban geomorphology is to investigate the changes to the natural landscape caused by human activities in cities (Cooke 1976; Cooke et al. 1982), and to consider humans as geomorphic agents, generating anthropogenic erosion and accumulation (Vergari et al., 2021; Campobasso et al., 2018). Urban geomorphology helps understanding the natural, historical, and anthropogenic landscape evolution, the changes imposed by settlements on natural geomorphological processes and geodiversity.

Here, we consider geomorphodiversity, a subset of geodiversity, as a representation of “the natural range, or diversity, of geological (rocks, minerals, fossils) geomorphological (landforms, topography, physical processes) and soil features” (Gray, 2013). In particular, we adopt the land surface diversity index (GmI) proposed by Burnelli et al., (2023) as a proxy for heterogeneity of land surface in Italy. The index is a discrete categorization of land surface diversity, embedding information on geology and digital elevation model-derived quantities.

Geomorphodiversity (Thomas, 2012a, b; Melelli et al., 2017; Burnelli et al., 2023) can be compared in urban areas with real-world urban geomorphological maps, and the comparison is an effective tool to analyze the impact of human activities on the Earth surface heterogeneity (Rito et al., 2022). In this work, we focus on the city of Rome, Italy, considering data collected with a geomorphological survey and mapping that has been going on for 20 years. Such survey has allowed the proposal of a model for the geomorphological classification of urban landscape (Della Seta et al., 2002, 2007; Del Monte et al., 2016; Luberti et al., 2018, 2019; Vergari et al., 2021, 2022). The geomorphological survey is still ongoing, and the urban geomorphological dataset of the metropolis describes the natural and anthropogenic processes and landforms, which shaped the city landscape. The dataset provides an unprecedented opportunity to study the complex effects of human activities, particularly those related to intense urbanization, on the spatial distribution of different levels of geomorphodiversity.

Within this context and with the available data, we tried to answer the following research questions:

I) how well can the GIS-based land surface diversity index represent the actual geomorphology of urban areas?

II) does anthropogenic morphogenesis contribute to geomorphodiversity?

To answer those questions, we compared the GmI of Italy with the landforms dataset of three areas describing Rome city's urban-rural gradient, "one of the techniques commonly used to investigate how urbanization is changing the ecological patterns and processes across the landscape" (McDonnell and Pickett, 1990; Hahs and McDonnell, 2006; McDonnell and Hahs, 2008).

A simple method allowed us the interpretation of the discrete geomorphodiversity values, as compared to the high-resolution map of landforms. We discuss the relationship between different geomorphodiversity values with the surveyed landforms, both natural and anthropogenic, to understand if diversity depends on the morphogenesis type. We further discuss whether GmI overestimates or underestimates (mismatch) the number and diversity of landforms observed in the real landscape.

2 Regional setting

Italy presents an outstanding variety of landscapes and landforms, due to its complex geological history and repeated climate changes. Its unique civilization history played a large role in shaping the landscapes through time (Marchetti et al., 2017). These characteristics are borne out in the geomorphodiversity index of Burnelli et al. (2023), which highlights a heterogeneous and interesting landscape. The same can be said about the Italian cultural landscape, shaped by the richness of historical metropolises, cities and villages, resulting from the 'joint works of nature and man' (Sauer, 1925).

The study area of this work is in the central part of the Italian peninsula, on the western side of Lazio region, encompassed by the municipality of Rome, the capital city of Italy (**Fig. 1**).

Rome arose south of the confluence between the Tiber and Aniene Rivers in the 8th century B.C. The elevation ranges from the minimum of 10-20m a.s.l. of the Tiber and Aniene floodplains to the maximum of 100-200m a.s.l., on the top of the volcanic plateau and the main structural relief.

A Plio-Pleistocene marine sedimentary basement characterizes the area (Funiciello and Giordano, 2008; Marra and Rosa, 1995). Volcanic, tectonic and glacio-eustatic processes interplayed in the area since the Middle Pleistocene. A volcanic plateau was generated by the Sabatini and Alban Volcanos (Karner et al., 2001; Giordano et al., 2006), formed during the Middle-Upper Pleistocene from several eruptive phases. It shows an alternance of effusive and pyroclastic rocks, and continental sediments (Funiciello and Giordano, 2008). Late Pleistocene fluvial erosion modeled the volcanic plateau, resulting in the historical hilly fluvial landscape of Rome deeply modified by three millennia of urbanization. A subsequent rise in sea level caused a depositional phase, during which alluvial deposits filled the valleys up to 60 meters (Ascani et al., 2008).

3 Materials and Methods

Materials used in this work are a geomorphological dataset, described in **Section 3.1**, and a land surface diversity index, in **Section 3.2**. The main method adopted here is a comparison of the two input maps, described in detail in **Section 3.3**; **Fig. 2** summarizes the procedure.

3.1 Geomorphological survey

The landscape of Rome is an outstanding example of urbanization characterized by the century-old stratification of urban expansion phases (Del Monte et al., 2013). Since its ancient time foundation, until the intense and progressive growth started after the Second World War and still ongoing (Del Monte et al., 2016), several kinds of human activities have been operating and generated anthropogenic erosion and accumulation, moving "tremendous amounts of soil and rock" (Hooke, 2000). The city progressively expanded over the centuries. During the Roman period, the expansion proceeded radially from the Tiber River, and later followed the directions of the main ancient Roman roads: to the east, before, and to the west, during the last 30 years, influencing the city urban-rural gradient.

The geomorphological investigation of such a deeply multi-layered and anthropized environment led Del Monte et al. (2016) to the proposal of the urban geomorphological survey method and subsequent improvements (Vergari et al., 2021). The survey is based on multitemporal data and materials analysis (*i.e.*, historical topography and orthophotos, satellite imagery, geognostic data), integrated by multidisciplinary investigations (*i.e.*, archaeological reports, historical archives, iconographical, artistic materials, etc.), and field survey. Geographical information system (GIS) software allows managing data overlay and operating processing of multitemporal data (Del Monte et al., 2016; Vergari et al., 2022), to understand the urban landscape evolution under natural and anthropogenic morphogenesis.

The mapping procedure relied on the guidelines for national geomorphological cartography (Campobasso et al., 2008), which classifies landforms following morphogenetic criteria, and considering both erosional and constructional processes. The case study of Rome demonstrates that in urban areas, natural morphogenetic processes are active in modeling landforms, and inactive landforms shaped by different morphogenetic conditions in the past exist as well. A third morphodynamic kind of natural landform is widespread in urban environment: modified natural landforms, modeled by natural processes but reshaped and altered by anthropogenic erosion and accumulation. Anthropogenic morphogenesis erases, buries, flattens natural morphologies or builds hills, generating new landforms and actively contributing to the evolution of the landscape under the influence of human activity. Moreover, geomorphological analysis of an urban area required innovative strategies for the detection and mapping human induced modifications to the topography, and anthropogenic landform classification, beyond the Italian national guidelines for geomorphological mapping (Vergari et al., 2022).

The natural and anthropogenic landform dataset adopted here is the preliminary result of the ongoing survey at 1:25,000 scale, and contains two major classes:

- Natural landforms – 2,507 elements, distinguished in 26 landform types;
- Anthropogenic landforms – 1,242 elements, distinguished in 21 landform types.

Natural and anthropogenic landforms are both distinguished in erosional and constructional and, in few cases, mixed landforms. The vector layers describing the landforms contain polygonal, point-like, and linear features.

We selected three areas, representative of different degrees of the urban-rural gradient: i) the natural landscape (NW area), ii) the modified natural landscape (NE area) and iii) the anthropogenic landscape (City center area). **Figure 1** shows boundaries of the three areas. Different choices for the definition of urban areas exist. For example, Bettencourt (2013) defined cities based on paved areas, and Alvioli et al. (2020) used a parameter-free approach to delineate cities boundaries starting from street junction information; both definitions are relevant for purposes other than scope of this work. Thus, the urbanization level and rural, urban-rural and urban conditions of the three areas are defined according to the Copernicus Dataset Urban Atlas Land Cover/Land Use (2018) classification for the Functional Urban Area (FUA; Dijkstra et al., 2019) of Rome. Urban Atlas classifies as urban land use (devoted to continuous or dense urban fabric, roads, industrial units, dump sites and leisure facilities) 69% of the city center area, 35% of the NE area, and 20% of the NW area.

3.2 Land surface diversity index at national and local scale

The land surface diversity index of Italy, GmI, is a quantitative geomorphodiversity index, obtained with a simple and objective method using geo-lithological information, a digital elevation model (DEM), and a few quantities derived from the DEM. The index provides an intuitive result, readily available for subsequent applications in different locations and at different scale resolutions.

The GmI map developed for Italy (Burnelli, et al. 2023) adopted EU-DEM (by Copernicus), at 25 m resolution, and the lithological map of Italy recently published by Bucci et al. (2022), at 1:100,000 scale. Topographic quantities such as slope, drainage network and landforms (namely, forms singled out by r.geomorphon, a model by Jasiewicz and Stepinski, 2013) were derived from the DEM.

The method used by Burnelli et al. (2023), extended from Benito-Calvo et al., (2009) and Melelli et al., (2017), consists of calculating partial diversity maps for the individual inputs, calculated with circular moving windows (QGIS and GRASS – GIS). The size of moving windows is a relevant parameter of the method. The resulting partial diversity maps were classified into five classes, combined into a single map (GIS sum), and reclassified into the final geomorphodiversity raster index, GmI, with a final spatial resolution of 500 m. In this work, we generated a GmI map with higher resolution, 25 m (**Fig. 3**) corresponding to the resolution of the EU-DEM, which is more suitable for the analysis at local scale than the published result.

The GmI consider the variability of landforms number, while other existing geodiversity assessment methods (*e.g.*, Hjort and Luoto, 2012; Tukiainen et al., 2016; Barančoková et al., 2023) explicitly consider landforms richness, namely the variability of different landforms. Since detailed geomorphological data are not continuously available for large area, these methods resort to Earth observation data and statistical modeling. On the other hand, the GmI adopted in this work considers morphometric types defined by the r.geomorphons model for landforms (Jasiewicz and Stepinski, 2013). For this reason, validation with real world geomorphological maps is of utmost importance.

Due to the local scale of the test areas (*cf*. **Fig. 1**), we argue that the size of GmI assessment in GIS (*i.e.*, size of moving windows to calculate diversity) should be pinned down by the size of the polygonal features resulting from the geomorphological survey. We selected a moving window radius using the square root of the mean area of the natural and the anthropogenic polygonal landforms.

3.3 Spatial distribution of natural and anthropogenic landforms

The spatial distribution of the number and of the diversity of point, linear and polygonal features was performed on a fishnet of 100×100 m cells, snapped to the GmI resampled at the same resolution. The analysis was carried out both separately and overall, for the natural and the anthropogenic geomorphological dataset, which resulted in six raster maps: number of natural landforms, number of different natural landforms (number of different landforms same as landforms richness in Hjort and Luoto, 2012; Tukiainen et al., 2016; hereafter, named natural/anthropogenic landform diversity), number of anthropogenic landforms, diversity of anthropogenic landforms, number of overall landforms and diversity of overall landforms. The maps were classified from 1 to 5 according to Jenks natural breaks, from the lowest to the highest number of landforms, in analogy with the method used for GmI (Burnelli et al., 2023).

3.4 Correspondence of GmI and diversity of observed landforms

We compared the GmI obtained at local scale (**Section 3.2**) with the six raster maps representing either the number and the diversity of landforms (**Section 3.3**), within the three surveyed areas (**Section 3.1**). To perform the comparison, we calculated the raster difference with the map algebra tool in QGIS and GRASS software. The results allowed us to test the effectiveness of the GmI concerning the geomorphological diversity observed in the field, in different contexts, where natural features and/or anthropic modifications exist. Therefore, this step enables us to detect positive or negative differences between the two inputs, and to investigate the potential of the index in urban areas, answering the question about how much anthropogenic morphogenesis contributes to geomorphodiversity or alter it.

In order to investigate the significance about the differences or similarities in the GmI versus observed landform number/diversity values in study areas, additional statistical analysis were desirable.

We have considered statistical tests, such as the Student's t-test, Mann-Whitney, and Kolmogorov-Smirnov tests. The t-test requires normally distributed variables, and all of the tests require continuous distributions, and use cumulative functions; none of the conditions are fulfilled, here. The issue is to figure out a test that accounts for both the spatial distribution and magnitude of the values. We considered Brier score *B*, considering for each grid cell a prediction, *Pi*, against an observed value, *Oi*, defined as:

$$B = \frac{1}{N}\sum_{i}^{N} (P_i - O_i)^2 , \tag{1}$$

This test is still not well defined, here, because it requires a binary prediction, and we have a five-valued prediction, instead. Thus, we considered the following simple test, which is inspired and generalizes the "true positive" and "false negative" indicators of confusion matrices. We extended the meaning of these indicators, considering "true positive" a prediction (GmI value) which matches the *i-th* class of an observation (maps obtained from geomorphological survey). We take into account all the five classes defining a synthetic indicator as follows:

$$I = \frac{1}{5}\sum_{i}^{5} \frac{TP_i}{TP_i + FN_i} , \tag{2}$$

Where *TPi* is the sum of true positives (prediction in the class $j=i$), for class *i*, across the study area, and *FNi* the sum of false negatives (prediction in a different class, $j\neq i$), for class *i*. With 5 possible values, the prediction is better than a random prediction if larger than 1/5. We have calculated the indicator *I* of Eq. (2) for the three different sectors in our study area (City Center, NO, and NE). Since we already noted that perfect match is seldom obtained, we generalized the expression in Eq. (2) considering as "positive" a prediction differing from the reference value by one unity, or by two unities.

4 Results

We discuss in separate paragraphs results of the geomorphological survey in three focus areas in Rome, the GmI calculated at local scale, the spatial distribution of natural and anthropogenic landforms, and how they compare with the GMI according to the methods developed in this work.

4.1 Natural and anthropogenic landforms in Rome

Figure 4 summarizes the results of the geomorphological survey. The natural landforms surveyed in Rome's landscape are fluvial, litho-structural, volcanic, and gravitational.

Examples of erosional fluvial landforms are through-shaped and flat-floor valleys, few examples of V-shaped valleys are present and rill and gully erosion, fluvial erosion scarps and crests are present. The process is active mainly in the rural and suburban area, to the NW and NE areas, meanwhile in the most urbanized area, City center, the valleys are inactive, due to culvert, or modified (Fig. 5a), because partially filled by anthropogenic deposits redefining the shape but not deleting the landform neither breaking the process. For this reason, in this work natural landforms modified by humans, but still recognizable, were grouped into the original natural morphogenetic process category. The wide Tiber River alluvial plain is the largest constructional fluvial landform of this kind, dividing the City center area in two parts, but several other fluvial landforms exist in the area. Litho-structural and volcanic landforms are related to the Pleistocene Sabatini and Alban Volcanos' activity: sub-horizontal structural surfaces shaped in the volcanic plateau deeply characterize the relief top, on both hydrographic right and left sides of the Tiber River. Landslides are concentrated on the marine sedimentary lithologies outcropping on the eastern slope of the main structural relief (western section of the city center area, Fig. 5b).

Anthropogenic landforms in the area correspond to constructional human activities such as infilling, dumping, channelizing, embanking, and erosional activities such as mining, quarrying, or excavations. Filling surfaces on ancient valleys and quarries are the most common constructional landforms, especially in the City center area. The infilled valleys are no longer recognizable in the landscape, as the fluvial process stopped, and the previous morphology (valley section) is recognizable only by paleo-morphology and historical landscape reconstruction. Artificial reliefs are also present because of dumping; there are examples of artificial hills or tabular reliefs due to walls retaining filling materials on hilltop. Many embankments are present, mainly related to the hydrological hazard management (*i.e.*, flooding). The Tiber River retaining walls are about 20 m high, built to embank the riverbanks to isolate the river beneath the city. Erosional anthropogenic landforms are excavation surfaces, made both for obtaining flat surfaces for urban fabric expansion (*i.e.*, slopes or saddle excavation, Fig. 5c) and for extraction of building rocks; man-made scarps, quarries, trenches are widespread.

Lastly, terraced slopes are mixed landforms of both anthropogenic erosion and accumulation. Slopes were terraced for building, reforestation, and agricultural activities.

4.2 Geomorphodiversity index at local scale

Figure 3 shows the GmI map at 25 m resolution at national scale. Values range from 1, the lowest value of land surface diversity, to 5, the highest. Areas with GmI = 1 represent 15.4% of Italy; value 2, 18.6%; value 3, 25.6%; value 4, 24.2%; value 5, 16.2%. The highest value of GmI is distributed in areas with larger apparent roughness, whereas the lowest values (1 and 2), amounting to about 34% overall, are generally distributed in gentle slope zones. The values 3 and 4 of GmI are represented throughout Italy, covering about 50% of the whole country.

In this work, to work at local scale, we adopted a version of the GmI map suited for comparison with the landforms observed in the field, alongside the national original GmI. For this reason, we considered the statistics of the natural and anthropogenic polygonal landforms. The absolute number of polygons, listed in **Table 1,** are similar, amounting to 616 natural and 629 anthropogenic features.

The average size of natural landform polygons' area is 0.17 km^2, while the anthropogenic is 0.06 km^2. In both cases, the vast majority of polygons are smaller than the average size. Only 15% of natural features are larger than the average size (91 polygons), whereas for 30% of anthropogenic landforms are larger than average (183 polygons). The standard deviation is large, 617,924 m^2 and 102,066 m^2 for natural and anthropogenic polygons, respectively, meaning that features are very different in size, particularly for natural features.

From the average polygon's radius size, which corresponds to 215 m and 121 m for natural and anthropogenic features, respectively, we obtain a moving window size to calculate a GmI at the local scale. They correspond to moving windows of 11 and 5 grid cells, respectively. We considered 11 grid cells as a lower limit to calculate the local version of GmI, at 25 m resolution. The map obtained using moving windows of 11 grid cells to calculate diversity was considered the most appropriate to validate the effectiveness of the index using the geomorphological elements existing in the test area, and it is shown in **Figure 6**.

4.3 Analysis of landforms spatial distribution

Figure 7 shows raster maps obtained considering either the number of landforms and the diversity of landforms in the geomorphological dataset (**Section 4.1**), within the three focus areas, separately for natural features (**Fig. 7a-b**), anthropogenic features (**Fig. 7c-d**), and overall (**Fig.7e-f**).

In the City center area, the natural features prevail in the western part (**Fig. 6a**), while in the NE area, most natural landforms are situated toward East, outside the Grande Raccordo Anulare, the annular road that encloses most of the urbanized area in Rome. In the NW zone, the distribution of this kind of features is more homogeneous compared to the other two focus areas. **Figure 7b** shows the diversity of natural elements. Except for a few sparse grid cells in the City center and in the NE area, the highest diversity of natural features (values 4 and 5) prevails in the NW focus area. In the City center area, value 3 is along the riverbank of Tiber River.

Figure 7c shows that the number of anthropogenic landforms prevail in the City center and in the western sector of the NE areas. In the NW sector, anthropogenic features are few, in the eastern part.

Figures 7d shows that the diversity of anthropogenic features is prominent in the City center and in the NE areas. In the NW area, the diversity of anthropogenic landforms is lower, with a few spots with values 2 and 3 in the eastern part.

Figures 7e and **7f** show the spatial distribution of the total number of features, natural and anthropogenic, and the total diversity of the geomorphological elements. The number of features is homogeneously distributed in all of the three areas, while the diversity of landforms prevails in the NW area, as long as in the left and right riverbanks of the Tiber River (City center) and the Aniene valley (NE area).

4.4. Comparing geomorphodiversity and observed landforms

Figure 8 shows the results of the comparison (raster difference in GIS) between the GmI (**Section 3.2**), and the raster maps derived from the landforms spatial distribution (**Section 4.3**) obtained separately for natural and anthropogenic landforms.

Table 2 displays the statistics of the above-mentioned comparison, within the three focus areas. The difference ranges from values +4 to -4. We reported the percentage of grid cells falling in each class, and within each area.

With respect to the number of natural landforms, the correspondence (raster difference = 0) between GmI and feature distribution is 14% and 13%, respectively in the NW and NE areas. In the City center, the correspondence is in 8% of the area. The remaining grid cells range from +1 to +4 values, meaning an overestimation by GmI of the number of landforms in the real-world landscape.

Concerning the diversity of natural landforms, the NW area shows the best correspondence, 29%, whereas in the City center and NE areas the percentage is 20% and 21%, respectively. The bigger discrepancy between GmI values and the raster map is in the City center area, where the percentage of grid cells with values ranging from +1 to +4 is 72%. The positive mismatch in the other two focus areas is lower, 43% of the NW area and 66% of the NE area.

The results of the comparison between GmI values and the distribution of the anthropogenic landforms show that in the NE correspondence is 18% of grid cells, 15% in the City center and 8% in the NW area. In all of the three focus areas, the mismatch ranges between values +1 and +4, (91% in the NW area and 77% in the City center and NE areas), which means that GmI overestimates the diversity of anthropogenic landforms in the real-world landscape.

With reference to the number of different anthropogenic features, the NW area shows the lowest correspondence with the GmI values, 8%, and the highest discrepancy, 91%. The City center and the NE areas show a better correspondence with GmI values, 15% and 17%, respectively. In all of the areas, the rest of the grid cells fall into mismatch values ranging from +1 to +4, with 91% of the NW area, 80% of the City center area and 77% of the NE area.

Figure 9 and **Table 3** report the results from the comparison between the GmI and the total number of landforms and the diversity of the landforms in the three focus areas.

Comparing the GmI with the total number of features, correspondence is 16% in the NW area, 19% in City center, and 22% in NE area. In general, the values ranging from -1 to -4 (GmI underestimating the real number of landforms) reach low percentages: 5% in the NW, 10% in the City center and NE areas. Conversely, the values from +1 to +4 are 79% of the NW area, 72% of the City center area and 67% of the NE area.

The results of the difference between the GmI and the total diversity of landforms shows correspondence in 23% of the NW area and 26% of the City center and of the NE areas. The negative mismatch (values from -1 to -4) is 10% of the NW area, 20% of the City center area, and 21% of the NE area. The positive mismatch (values from +1 to +4), reflecting an overestimation of landscape variability by GmI, is 67% of the NW area, 55% of the City center area, and 52% of the NE area.

The statistical significance of the comparison between GmI and number/diversity of observed landforms is listed in **Table 4**. Results confirm that cell-by-cell match between the “prediction” and the “observation” are slightly larger than a random distribution but considering a mismatch by one unity substantially increases the value of the indicator of Eq. (2). Considering that the pair-wise comparisons involve maps obtained from completely different data sources, we maintain that the result is meaningful.

5. Discussion

We presented results of the comparison of a model for land surface diversity, the GmI in **Fig. 3**, with the real-world landscape of Rome, across the urban-rural gradient, represented by an accurate geomorphological map. The effort aims at answering the research questions “how much does anthropogenic morphogenesis contribute to geomorphodiversity? Does it alter geomorphodiversity in urban environment?”.

In the following, we discuss results in three separate sections, devoted to discussing (i) a characterization individual landform types with GmI values, to understand whether natural or anthropogenic landforms relate to land surface diversity (**Section 5.1**), (ii) calculation of the mismatch between GmI and a corresponding index, calculated from the spatial distribution of the landforms for the geomorphological map (**Section 5.2)**; (iii) discussion of the result in relation to the existing literature on urban geodiversity assessment (**Section 5.3**).

5.1 GmI values characterizing individual landform types

The landforms having largest impact on the real-world surface diversity are the polygonal features of the geomorphological dataset (consisting of point, linear, and polygonal geometries). In fact, polygonal features are spatially the most consistent in the geomorphological database of Rome, thus the most representative: they describe well the spatial distribution of geomorphological processes, especially with respect to anthropogenic transformations to the landscape and are therefore significant for the investigation of geomorphodiversity in urban environments. For this reason, we analyzed the spatial distribution of GmI values, and their spatial relationship with natural and anthropogenic polygonal landforms.

Table 5 shows statistics of the joint distribution of GmI values and natural landform types: focusing on the area covered by individual landform types, we analyzed the GmI mean values within the landform polygons.

The GmI is higher in gravitational accumulation (landslide bodies, 4) and fluvial (alluvial fan, 3.89) landforms, where the deposits generated geomorphic features with relief that stands out against the adjacent, more monotonous morphology.

As expected, the lowest GmI values correspond to flat morphology, within the vast sub-horizontal structural surfaces and floodplains (mean GmI 2.75), and in regions with slightly inclined but regular surfaces subject to diffuse runoff and solifluction (3-3.30). Where the summit structural surfaces are degraded, morphology becomes irregular and GmI values increase (sub-structural surface, 3.39).

Medium-high GmI values are in the vast alluvial plains of the Tiber River and its tributaries (mean GmI 3.37). Intuitively, vast flat morphologies should be less "geomorphodiverse", in line with rather homogeneous terrain. This can be understood considering the drainage density input in the calculation of GmI, which likely contributes with unrealistic values in these regions and leads to a slight overestimation of the index values.

Table 6 shows the overlap degree between GmI values and the anthropogenic landforms. The findings are interesting, in fact they highlight that GmI well describes the morphological characteristics resulting from anthropogenic modifications of the relief.

The classification of anthropogenic landforms into erosion, accumulation, and mixed features does not seem to determine a specific trend in the geomorphodiversity values. Anthropogenic modifications to the relief can simplify or enrich the morphology, regardless of the accumulation or erosion nature of the processes, and these variations are well described by the GmI values.

The highest GmI values correspond to morphological features enriched by anthropogenic activities like building artificial hills (mean GmI 3.85), landfilling or dumping areas (3.76), or terracing hillslopes for building or agricultural activity (3.48 and 3.84, respectively). Medium-high GmI values correspond to excavation surfaces (mean GmI 3.40), and lower values are in locations where human activity has reduced the surface ruggedness, for example filling valleys (mean GmI 2.84) or other depressions (filling in an ancient quarry, 2.77), or leveling previous reliefs for extraction activities (quarry/mine, 2.63) or construction purposes.

The histograms in **Figure 10** summarize the percentage of each focus area covered by each GmI class. The highest geomorphodiversity is in the NW area, where about 80% is in medium-high GmI classes. This is likely related to the large number of fluvial landforms, thanks to a well-developed drainage network, unaffected by valleys filling and morphology flattening. These landforms, together with run-off and gravitational processes, describe active natural morphodynamics in this mostly rural area, and that is borne out by the calculated GmI values.

In the City center, 72% of the area is in medium-high GmI classes. The area is rich in gravitational accumulation and fluvial landforms, among natural landforms, and landfill, dumps and terraced slopes are widespread in this markedly urban area. According to **Table 5**, the mentioned landform types increase geomorphodiversity and that is borne out in GmI values. In the City center area, filling surfaces in ancient quarries and valleys, embankments and infills flattened the morphology, that is also manifest from lower GmI values, with respect to the NW area.

The NE area is covered for 63% by medium-high GmI classes. The remaining, lower-GmI region, is due to the balanced presence of roughening and flattening geomorphic features, both natural and anthropogenic (see the spatial distribution of the natural and anthropogenic landforms in **Fig.7**), either increasing or reducing the complexity of the morphology. The transitional condition of this urban-rural territory is well described by the GmI values.

5.2 Matching the diversity of landforms with GmI values

Table 7 summarizes the results described in **Section 4.4** about differences between GmI and natural and anthropogenic landforms (considered separately), and between GmI and total landforms, in each focus area.

Considering as not significant a difference between -3 and 3, the results highlight a good correspondence with respect to the number and diversity of real landforms; overestimation of geomorphodiversity is less common, and underestimation is very low (1%) or zero, in each focus area. We discuss the spatial distribution of values and types of landscape features involved.

In the NW area, correspondence (raster difference = 0) of GmI and the number of observed natural landform number covers 73% of the area, while correspondence between GmI and the diversity of natural landforms covers 94% of the area. For anthropogenic landforms, the difference is positive in about 50% of the area. Considering natural landforms separately to anthropogenic ones, in the NW area the GmI is overestimated with respect to the number of natural landforms (27%), especially with respect to the number and diversity of anthropogenic landforms. Considering the total number and diversity of landforms, correspondence covers 79% and 87% of the area, respectively.

We stress that the spatial distribution of GmI values describe correctly both natural and anthropogenic landforms. In the NW area, the overestimation of anthropic landforms by GmI is not due to the landforms distribution itself, but to the fact that there is practically none, there. In fact, considering the aggregated number and variability of natural and anthropogenic landforms, the discrepancy is minimal, as no regions exist with no landforms at all. Therefore, the discrepancy is not due to anthropogenic landforms nor to a poor accuracy of the elevation model, or the GmI model, in the built areas.

In the City center area, correspondence with the number of natural landforms number covers 67% of the area, and 84% in the case of diversity of natural landforms. For anthropogenic landforms, correspondence is in 70% and 71% of the area for the number and diversity, respectively. Overestimation of landforms by GmI covers about 30% of the area, it mainly concerns the number of landforms, both natural and anthropogenic, while overestimation is more common for anthropogenic landforms diversity than natural ones. Overestimation occurs in regions with low landform density. Our interpretation is that the high values of GmI are due to substantial relief in such locations, contained in the slope contribution to GmI, which increase geomorphodiversity regardless of actual presence of specific, mapped landforms. The correspondence between GmI and the total number and diversity of landforms is good; it covers 80% and 90% of the area, respectively. The City center area is characterized by intense urbanization and abundant anthropogenic landforms, thus the overall good correspondence suggests that both natural and anthropogenic landforms contribute to geomorphodiversity in this urban area.

The NE area shows the best correspondence between GmI and anthropogenic landforms, as well as total number and total diversity of landforms. Moreover, the NE area shows the lowest overestimation of landforms by GmI. Thus, we can conclude that the good balance in natural and anthropogenic landforms distribution confirms the same contribution to geomorphodiversity of the two types of landforms.

5.3 Approaches and results about urban geodiversity in scientific literature

The comparison of the GmI separately with natural and anthropogenic landforms in **Section 5.2** showed that the land surface diversity index GmI is not influenced by the distribution in the real landscape of anthropogenic or natural landforms. Thus, both natural and anthropogenic processes contribute to geomorphodiversity in the three areas with different urbanization level considered here. Instead, individual types of natural or anthropogenic landforms contribute differently to the GmI, as described in **Section 5.1**.

In this study, geomorphodiversity is considered as a subset of geodiversity and a proxy for the quantification of the Earth surface heterogeneity, to which anthropogenic activities deeply impact in urban environments.

The approach based on the comparison of geomorphodiversity with real-world urban geomorphological maps in urban areas resulted an effective tool to analyze the impact of human activities on geomorphological processes. That was seldom considered in quantifying the Earth surface heterogeneity in the literature. The results leave room for interpretation. In fact, human activities are usually considered to have a negative impact from environmental and ecological point of view. We have shown that anthropogenic modifications to the relief can increase or decrease the complexity of the landscape, and, consequently, decrease or increase local surface diversity.

Scientific literature on geodiversity studies investigating urban environment propose approaches very different to the one in this study. Geomorphology is predominant in geodiversity perception (Hubert et al., 2019) and it is also the main geodiversity component having ecological significance, at local scale especially (Tukiainen et al., 2019).

A first attempt in urban geodiversity assessment is in Ilić et al. (2016). They apply a quantitative geodiversity index to the Belgrade city area, based on the number of different abiotic elements in specific spatial unit. They consider roughness to quantify geomorphology assessment and discuss the anthropogenic impact comparing high geodiversity classes with the location of protected areas. Santos et al. (2017) used a grid-based geodiversity index to identify the most geodiverse areas of the municipality of Armação dos Búzios (Brazil), comparing the geodiversity classes with the urban expansion map over a 30-year time. The study considered geology, geomorphology, soil and hydrography, and a geomorphological map of the city, mainly describing morphological types. Combining the geodiversity and urban expansion map, they quantified the percentage of area impacted by urban growth in each geodiversity index class.

The two studies described above are the only examples of quantitative geomorphodiversity assessment in urban environments. However, they lack comparison with real landforms, particularly anthropogenic ones. Thus, they omit the assessment of the anthropogenic impact on Earth's surface diversity.

Our study enriches the scientific literature on the quantitative assessment of urban geodiversity. The strength of our approach lies in its comparison with actual geomorphology, especially anthropogenic landforms, which is fundamental for assessing the heterogeneity of the Earth's surface in urbanized environments.

Other examples in literature are not urban geodiversity quantitative assessment, but EGVs (Essential Geodiversity Variables) and ES (Ecosystem Services) assessment. All these studies (da Silva and do Nascimento, 2020; Reverte et al., 2020; Balaguer et al., 2022, 2023) consider landforms as essential geodiversity variables, but they used morphologies, geomorphological processes, and morphodynamical domains, instead of explicitly considering landforms. Furthermore, they considered anthropogenic morphogenesis only marginally, just contemplating technogenic deposits, while anthropogenic impacts assessment analyzes land use changes impact on ES provided by geodiversity.

Rito et al. (2022) modified and applied a previous version of the GmI (Melelli et al., 2017) to the city of Puerto Madryn (Argentina). To evaluate anthropogenic impact, they qualitatively compared urban expansion analysis with landforms distribution, discussing each landform type, but neglecting anthropogenic landforms.

Thus, our work is the first attempt to quantitatively relate the geomorphodiversity of an area with the real-world distribution of surveyed anthropogenic landforms, to objectively test the capability of the GmI of measuring also the land surface diversity due to human-induced modifications.

6. Conclusions

Research studies on urban geodiversity are very few and, to the best of our knowledge, this work analyzed urban geomorphodiversity in relation with the surveyed geomorphology, interpreting the distribution of diversity classes based on the characteristics of the real-world landscape.

Based on our results, we can answer the question posed in the title and introduction in the following way: anthropogenic morphogenesis alters geomorphodiversity in urban environments, as much as natural morphogenesis does.

In fact, anthropogenic landforms do not decrease surface diversity, as one might expect taking for granted that human activities have a huge impact on the landscape. Instead, the impact on the land surface diversity depends on the types of anthropogenic processes that model an area and produce new landforms, at least as much as natural processes. Landforms resulting from flattened morphology correspond to decreased landscape complexity, and consequently on a reduced geomorphodiversity. Landforms generating new relief correspond to increased geomorphodiversity.

Our results showed that the considered GmI approach can detect the land surface diversity due to both natural and anthropogenic morphogenesis. Though in this work we considered a scaled-down version of a national-scale GmI map, one interesting point to understand is whether the process can be extended further to consider multitemporal and different resolution DEMs, accounting for additional landform types, using more landscape metrics (i.e. Sofia et al., 2014) and, potentially, additional high-resolution information.

The current trend of population growth at global level and increasing urban sprawl supports efforts should include urban geomorphodiversity and geomorphological studies at a local scale, studying real-world natural and anthropogenic landforms, and considering the impact of human activities in a critical and constructive way. This conclusion is challenging and supports the planning of human activities in urban areas that favor anthropogenic processes which increase geodiversity and Earth's surface heterogeneity rather than diminishing it.

CRediT authorship contribution statement

Martina Burnelli: Conceptualization, Data curation, Formal analysis, Investigation, Methodology, Software, Visualization, Roles/Writing - original draft and Writing - review & editing; **Alessia Pica**: Conceptualization, Data curation, Formal analysis, Investigation, Methodology, Visualization, Roles/Writing - original draft and Writing - review & editing; **Maurizio Del Monte**: Conceptualization, Funding acquisition, Project administration, Resources and Writing - review & editing; **Michele Delchiaro**: Data curation, Investigation, Visualization and Writing - review & editing; **Laura Melelli**: Conceptualization, Formal analysis, Funding acquisition, Investigation, Methodology, Project administration, Resources and Writing - review & editing; **Francesca Reame**: Data curation, Investigation and Writing - review & editing; **Francesca Vergari**: Conceptualization, Formal analysis, Investigation, Methodology, Visualization and Writing - review & editing; **Massimiliano Alvioli**: Conceptualization, Data curation, Formal analysis, Funding acquisition, Investigation, Methodology, Project administration, Resources, Software, Supervision and Writing - review & editing.

Acknowledgements

We are grateful to two anonymous reviewers for their deep and stimulating revision of the manuscript, as well as to the Editor for their meticulous and supportive editorial guidance.

Funding

Alvioli M. and Melelli L. partially supported by project by Project "URGERE: URban Geodiversity for a Resilient Environment" 2022M7EP3M_PE10_PRIN2022 - PNRR M4.C2.1.1 - Funded by the European Union – Next Generation EU - CUP: B53D23007260006.

Del Monte M., Delchiaro M., Pica A., Reame F. and Vergari F. partially supported by the funds of the CARG – Project – Geological Map of Italy 1:50,000.

References

Alvioli, M., 2020. Administrative boundaries and urban areas in Italy: A perspective from scaling laws. Landscape and Urban Planning, 204, 103906. https://doi.org/10.1016/j.landurbplan.2020.103906.

Ascani, F., Bozzano, F., Buccellato, A., Del Monte, M., Matteucci, R., Vergari, F., 2008. Evoluzione del paesaggio e antiche vie di drenaggio nell'area de 'Il Castellaccio' (Roma) da indagini geologiche, geomorfologiche e archeologiche. Geologica Romana 41, 93–116. Available at: https://www.dst.uniroma1.it/VolumeXLI (accessed 14 May 2024).

Balaguer P.L., da Glória Motta Garcia M., Reverte F.C., Maria de Almeida Leite Ribeiro L., 2023. To what extent are ecosystem services provided by geodiversity affected by anthropogenic impacts? A quantitative study in Caraguatatuba, Southeast coast of Brazil, Land Use Policy 131, 106708, ISSN 0264-8377, https://doi.org/10.1016/j.landusepol.2023.106708.

Balaguer, P. L., da Glória Motta Garcia, M. and Maria de Almeida Leite Ribeiro, L., 2022. Combined Assessment of Geodiversity As a Tool to Territorial Management: Application to Southeastern Coast of State of São Paulo, Brazil. Geoheritage 14, 60. https://doi.org/10.1007/s12371-022-00696-7.

Barančoková, M., Hutárová, D., Nikolaj, M., 2023. Quantitative Assessment of Geodiversity for Conservation Purposes in Slovenské rudohorie Mountains (Slovakia). Land 12, 1650. https://doi.org/10.3390/land12091650.

Barančoková M., Hutárová D., Nikolaj M., 2023. Quantitative Assessment of Geodiversity for Conservation Purposes in Slovenské rudohorie Mountains (Slovakia). Land 12, 1650. https://doi.org/10.3390/land12091650.

Bettencourt, L.M.A., 2013. The origins of scaling in cities. Science 340, 682 1438–1441. https://doi.org/10.1126/science.1235823.

Bojinski, S., Verstraete, M., Peterson, T., Richter, C., Simmons, A., Zemp, M., 2014. The Concept of Essential Climate Variables in Support of Climate Research, Applications, and Policy. Bulletin of The American Meteorological Society 95 (9), 1431-1443. https://doi.org/10.1175/BAMS-D-13-00047.1.

Bucci, F., Santangelo, M., Fongo, L., Alvioli, M., Cardinali, M., Melelli, L., and Marchesini, I., 2022. A new digital lithological map of Italy at the 1:100 000 scale for geomechanical modelling. Earth Syst. Sci. Data 14, 4129–4151, https://doi.org/10.5194/essd-14-4129-2022.

Burnelli, M., Melelli, L., Alvioli, M., 2023. Land surface diversity: A geomorphodiversity index of Italy. Earth Surface Processes and Landforms. https://doi.org/10.1002/esp.5679.

Burnelli, M., Melelli, L., Alvioli, M., 2024. High-resolution geomorphodiversity and anthropization indices of Italy for urban geomorphology. Under review (this volume).

Campobasso, C., Carton, A., Chelli, A., D'Orefice M., Dramis, F., Graciotti, R., Pellegrini, L., 2018. Aggiornamento ed Integrazioni delle Linee Guida della Carta Geomorfologica d'Italia alla Scala 1:50.000; ISPRA: Rome, Italy. Available at: https://www.isprambiente.gov.it/files2023/pubblicazioni/periodici-tecnici/q13_fascicolo_ii-ver1-0-1.pdf (accessed 14 May 2024).

CARG Project - Geologic and geothematic cartography https://www.isprambiente.gov.it/it/progetti/cartella-progetti-in-corso/suolo-e-territorio-1/progetto-carg-cartografia-geologica-e-geotematica/index.

Cooke, R.U., 1976. Urban geomorphology. Geographical Journal 142(1), 59–65. https://doi.org/10.2307/1796025.

Cooke, R.U., Brunsden, D., Doornkamp, J.C., Jones, D.K.C., 1982. Urban geomorphology in Drylands. Oxford University Press, Oxford, 324 pp. ISBN 019823239X

da Silva, M.L.N., do Nascimento, M.A.L., 2020. Ecosystem Services and Typology of Urban Geodiversity: Qualitative Assessment in Natal Town, Brazilian Northeast. Geoheritage 12, 57. https://doi.org/10.1007/s12371-020-00479-y.

Del Monte, M., Fredi, P., Pica, A., Vergari, F., 2013. Geosites within Rome City center (Italy): a mixture of cultural and geomorphological heritage. Geografia Fisica e Dinamica Quaternaria 36(2), 241-257. https://doi.org/10.4461/GFDQ.2013.36.20

Del Monte, M., D'Orefice, M., Luberti, G. M., Marini, R., Pica, A., Vergari, F., 2016. Geomorphological classification of urban landscapes: the case study of Rome (Italy). Journal of Maps 12(1), 178-189. https://doi.org/10.1080/17445647.2016.1187977.

Della Seta M., Del Monte M., 2007. Pericolosità per inondazione fluviale lungo il corso urbano del Fiume Aniene. In: Scritti per Alberto De Blasi, pp. 517-529. Pàtron, Rome. EAN 9788855528764.

Della Seta M., Del Monte M., Fredi P., Marra F., Pantani G., 2002. Caratteri morfostrutturali del settore in riva destra del Fiume Tevere nell'area urbana di Roma. In: Geologica Romana 36:(2002), pp. 105-122. - ISSN 0435-3927.

Dijkstra, L., Poelman, H., Veneri, P., 2019. The EU-OECD definition of a functional urban area. OECD Regional Development Working Papers, No. 2019/11, OECD Publishing, Paris, https://doi.org/10.1787/d58cb34d-en.

Funiciello, R., Giordano, G., 2008. La nuova carta geologica di Roma: litostratigrafia e organizzazione stratigrafica. In: Funiciello R., Praturlon A., Giordano G. (Eds) La geologia di Roma dal centro storico alla periferia. Memorie Descrittive della Carta Geologica d'Italia 80 (1), 39–85

Giordano, G., De Benedetti, A., Diana, A., Daudioso, F., Marasco, F., Miceli, M., Funiciello, R., 2006. The Colli Albani mafic caldera (Roma, Italy): Stratigraphy, structure and petrology. Journal of Volcanology and Geothermal Research 155, 49–80.

Gray, M., (2013. Geodiversity: valuing and conserving abiotic nature, 2nd Edition. Chichester, West Sussex PO19 8SQ, England: Wiley-Blackwell. 512 pp. ISBN: 978–0–470-74215-0

Grenier, M., Lantz, N., Soulard, F., Wang, J., 2020. The Use of Combined Landsat and Radarsat Data for Urban Ecosystem Accounting in Canada. Statistical Journal of the IAOS 36, 823–839. https://doi.org/10.3233/SJI-200663.

Hahs, A.K., McDonnell, M.J., 2006. Selecting independent measures to quantify Melbourne's urban–rural gradient. Landscape and Urban Planning Volume 78, (4), 435-448, ISSN 0169-2046. https://doi.org/10.1016/j.landurbplan.2005.12.005.

Hjort, J., Luoto, M., 2012. Can geodiversity be predicted from space? Geomorphology 153, 74-80. https://doi.org/10.1016/j.geomorph.2012.02.010.

Hooke, R. L., 2000. On the history of humans as geomorphic agents. Geology 28(9), 843–846. https://doi.org/10.1130/0091-7613(2000)28%3C843:OTHOHA%3E2.0.CO;2.

Hubert, I., Reynard, E., Carcaud, N., 2019. Donner à voir la géodiversité de la région grenobloise et dépasser le clivage ville / montagne à travers le prisme du paysage et de ses représentations. Géomorphologie Relief, Processus, Environnement. 25 (4). Géodiversité représentée. https://doi.org/10.4000/geomorphologie.13701.

Ilić, M. M., Stojković, S., Rundić, L., Ćalić, J., Sandić, D., 2016. Application of the geodiversity index for the assessment of geodiversity in urban areas: An example of the Belgrade City area, Serbia. Geologia Croatica 69 (3). https://doi.org/10.4154/gc.2016.27.

Jasiewicz, J., Stepinski, T.F., 2013. Geomorphons — a pattern recognition approach to classification and mapping of landforms. Geomorphology 182, 147–156. https://doi.org/10.1016/j.geomorph.2012.11.005.

Karner, D. B., Marra, F., Renne, P. R., 2001. The history of the Monti Sabatini and Alban hills volcanoes: Groundwork for assessing volcanic-tectonic hazards for Rome. Journal of Volcanology and Geothermal Research 107, 185–215. https://doi.org/10.1016/S0377-0273(00)00258-4

Kubalíková, L., Kirchner, K., Bajer, A., 2017. Secondary geodiversity and its potential for urban geotourism: a case study from Brno city, Czech Republic. Quaestiones Geographicae 36, 63–73. https://doi.org/10.1515/quageo-2017-0024.

Kubalíková, L., Bajer, A., 2018. Geotourism within urban areas: new ways of promotion of natural and cultural heritage (case study from Brno City). In: Svobodová H (ed) Proceedings of 25th Central European Conference - Useful Geography: Transfer from Research to Practice. Masarykova univerzita, Brno, 462–472. https://doi.org/10.5817/CZ.MUNI.P210-8908-2018.

Kubalíková, L., Kirchner, K., Kuda, F., Machar, I., 2019. The role of anthropogenic landforms in sustainable landscape management. Sustainability 11, 4331. https://doi.org/10.3390/su11164331.

Kubalíková, L., Drápela, E., Kirchner, K., Bajer, A., Balková, M., Kuda, F., 2021. Urban geotourism development and geoconservation: is it possible to find a balance? Environ Sci & Policy 121, 1–10. https://doi.org/10.1016/j.envsci.2021.03.016.

Luberti, G.M., Vergari, F., Marini, R., Pica, A., Del Monte, M., 2018. Anthropogenic modifications to the drainage network of Rome (Italy): the case study of the Aqua Mariana. Alpine and Mediterranean Quaternary, 31 (2), 1 - 14.

Luberti, G.M., Vergari, F., Pica, A., Del Monte, M., 2019. Estimation of the thickness of anthropogenic deposits in historical urban centres: An interdisciplinary methodology applied to Rome (Italy). The Holocene Vol 29 (1), https://doi.org/10.1177/0959683618804630

Marra, F., Rosa, C., 1995. Stratigrafia e assetto geologico dell'area romana – In: La geologia di Roma: il centro storico. Memorie Descrittive della Carta Geologica d'Italia 50, 49–118.

Marchetti, M., Soldati, M., Vandelli, V., 2017. The Great Diversity of Italian Landscapes and Landforms: Their Origin and Human Imprint. In: Soldati, M., Marchetti, M. (eds.) Landscapes and Landforms of Italy. World Geomorphological Landscapes. Springer, Cham. https://doi.org/10.1007/978-3-319-26194-2_2.

McDonnell, M.J., Pickett, S.T.A., 1990. Ecosystem structure and function along urban rural gradients: An unexploited opportunity for ecology. Ecology 71, 1232–1237. https://doi.org/10.2307/1938259.

McDonnell, M.J., Hahs, A.K., 2008. The use of gradient analysis studies in advancing our understanding of the ecology of urbanizing landscapes: current status and future directions. Landscape Ecology 23, 1143–1155. https://doi.org/10.1007/s10980-008-9253-4.

Melelli, L., Vergari, F., Liucci, L., Del Monte, M., 2017. Geomorphodiversity index: Quantifying the diversity of landforms and physical landscape. Science of the Total Environment 584, 701-714. https://doi.org/10.1016/j.scitotenv.2017.01.101.

Moradipour, F., Moghimi, E., Beglou, M.J., Yamani, M., 2020. Assessment of Urban Geomorphological Heritage for Urban Geotourism Development in Khorramabad City, Iran. Geoheritage 12, 40. https://doi.org/10.1007/s12371-020-00466-3.

Mucivuna, V.C., Reynard, E., Garcia, M.D.G.M., 2019. Geomorphosites assessment methods: comparative analysis and typology. Geoheritage 11, 1799-1815. https://doi.org/10.1007/s12371-019-00394-x.

Pica, A., Vergari, F., Fredi, P., Del Monte, M., 2016. The aeterna urbs geomorphological heritage (Rome, Italy). Geoheritage 8, 31–42. https://doi.org/10.1007/s12371-015-0150-3.

Pica, A., Luberti, G.M., Vergari, F., Fredi, P., Del Monte, M., 2017. Contribution for an urban geomorphoheritage assessment method: proposal from three geomorphosites in Rome (Italy). Quaestiones Geographicae 36, 21–36. https://doi.org/10.1515/quageo-2017-0030.

Pica, A., Reynard, E., Grangier, L. Kaiser, C., Ghiraldi, L., Perotti, L., Del Monte, M., 2018. GeoGuides, urban geotourism offer powered by mobile application technology. Geoheritage 10, 311–326 https://doi.org/10.1007/s12371-017-0237-0.

Rebele, F., 1994. Urban ecology and special features of urban ecosystems. Global Ecology and Biogeography Letters 4(6), 173–187. https://doi.org/10.2307/2997649.

Reverte, F. C., Garcia, M. G. M., Brilha, J., Pellejero, A. U., 2020. Assessment of impacts on ecosystem services provided by geodiversity in highly urbanised areas: a case study of the Taubaté Basin, Brazil. Environmental Science & Policy 112, 91-106. https://doi:10.1016/j.envsci.2020.05.015.

Rito, C., Boretto, G., Bazzano, G., Cioccale, M., 2022. Assessment of geomorphodiversity and the impacts of urban growth in Puerto Madryn, Patagonia, Argentina. Journal of South American Earth Sciences 119, 104018. https://doi.org/10.1016/j.jsames.2022.104018.

Sabogal, A., 2021. Urban Ecology. In: Urban Ecology. Sustainable Development Goals Series. Springer, Cham. https://doi.org/10.1007/978-3-030-69905-5_7.

Santos, D.S., Mansur, K.L., Gonçalves, J.B., Arruda, E.R., Manosso, F.C., 2017. Quantitative assessment of geodiversity and urban growth impacts in Armação dos Búzios, Rio de Janeiro, Brazil, Applied Geography 85, ISSN 0143-6228, https://doi.org/10.1016/j.apgeog.2017.03.009.

Sauer, C. O., 1925. The morphology of landscape. University of California pubblications in Geography 2, 19-53.

Schrodt, F., 2019. Opinion: to advance sustainable stewardship, we must document not only biodiversity but geodiversity. Proc. Natl. Acad. Sci. USA 116(33), 155–158. https://doi.org/10.1073/pnas.1911799116.

Schrodt, F., Vernham, G., Bailey, J., Field, R., Gordon, J. E., Gray, M., Hjort, Jan and Hoorn, C., Hunter Jr., M. L., Larwood, J., Lausch, A., Monge-Ganuzas, M., Miller, S., van Ree, D., Seijmonsbergen, A. C., Zarnetske, P. L., Daniel

Kissling, W., 2024. The status and future of essential geodiversity variables. Phil. Trans. R. Soc. A 382, 20230052. https://doi.org/10.1098/rsta.2023.0052.

Sofia, G., Marinello, F., Tarolli, P., 2014. A new landscape metric for the identification of terraced sites: the Slope Local Length of Auto-Correlation (SLLAC). ISPRS Journal of Photogrammetry and Remote Sensing 96, 123-133. https://doi.org/10.1016/j.isprsjprs.2014.06.018.

Thomas, M. F., 2012a. A geomorphological approach to geodiversity - its applications to geoconservation and geotourism. Quaestiones Geographicae 31 (1), 81-89. https://doi.org/10.2478/v10117-012-0005-9.

Thomas, M. F., 2012b. Geodiversity and Landscape Sensitivity: A Geomorphological Perspective. Scottish Geographical Journal 128(3–4), 195–210. https://doi.org/10.1080/14702541.2012.725863.

Tukiainen H., Bailey J. J., Field R., Kangas K., Hjort J., 2016. Combining geodiversity with climate and topography to account for threatened species richness. Conservation Biology 31 (2), 364-375. https://doi.org/10.1111/cobi.12799.

Tukiainen, H., Kiuttu, M., Kalliola, R., Alahuhta, J., Hjort, J., 2019. Landforms contribute to plant biodiversity at alpha, beta and gamma levels. J. Biogeogr. 46, 1699-1710, https://doi.org/10.1111/jbi.13569.

United Nations, Department of Economic and Social Affairs, Population Division, 2012. World urbanization prospects: The 2011 revision. URL: http://esa.un.org/unpd/wup/index.html

Urban Atlas Land Cover/Land Use 2018 (vector), Europe, 6-yearly; European Union's Copernicus Land Monitoring Service information. https://doi.org/10.2909/fb4dffa1-6ceb-4cc0-8372-1ed354c285e6

Vergari, F., Luberti, G.M., Pica, A., Del Monte, M., 2021. Geomorphology of the historic centre of the Urbs (Rome, Italy). Journal of Maps 17(4), 6-17. https://doi.org/10.1080/17445647.2020.1761465

Vergari, F., Pica, A., Brandolini, P., Melelli, L., Del Monte, M., 2022. Geomorphological classification of the landscape in urban areas. Hints from some study cases in Italy. Rendiconti Online Della Società Geologica Italiana 57, 33-39.

10 Figures and Tables

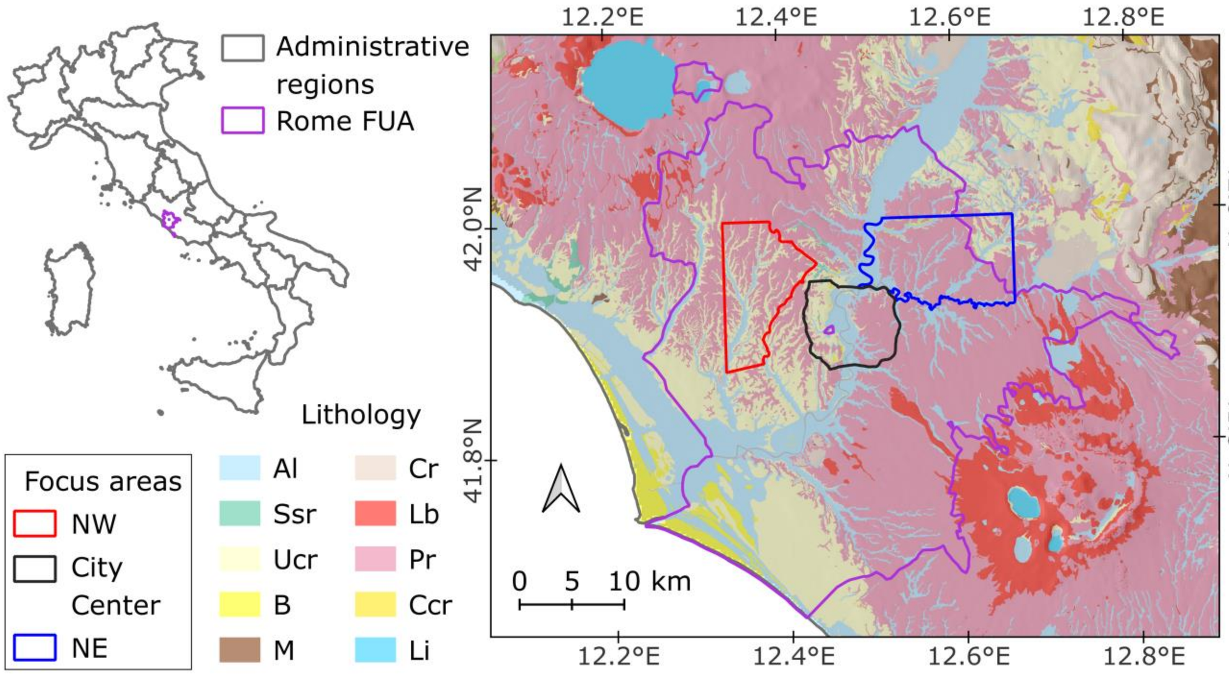

Figure 1. Location of the study area. The polygons describe the overall boundary of the core area of Rome Functional Urban Area (FUA; Dijkstra et al., 2019) (purple), and three focus areas considered in this work (black, blue, red). Lithological information from Bucci et al. (2022): Al – Alluvial and marine deposits; Ucr – Unconsolidated clastic rocks; Cr – Carbonate rocks; Ssr – Siliciclastic sedimentary rocks; Ccr – Consolidated clastic rocks; Pr – Pyroclastic rocks; Lb – Lavas and basalts; M – Marlstone; Li - Lakes; B - Beach deposits. All maps used in this work are in ETRS89-extended / LAEA Europe projected reference system (EPSG 3035); the figures show WGS84 (EPSG 4326) coordinates for ease of interpretation.

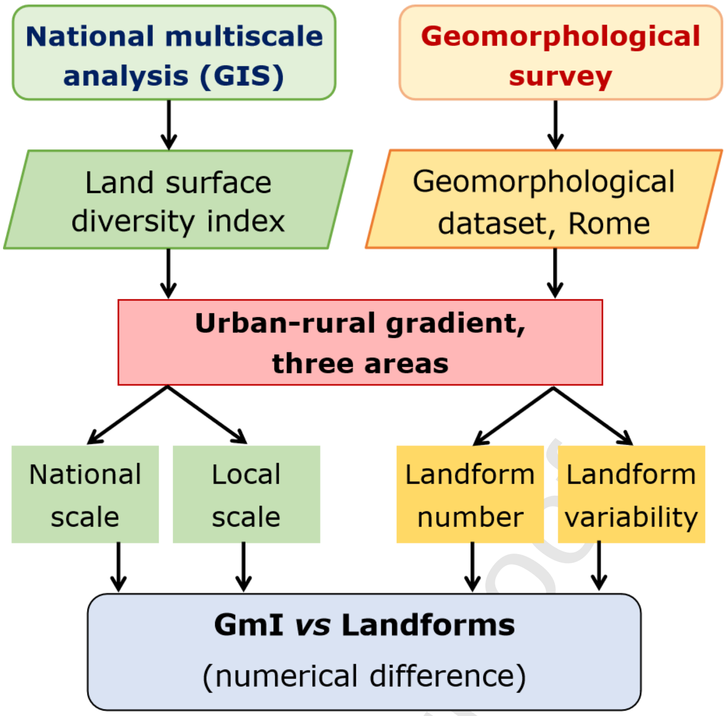

Figure 2. Flowchart describing the steps of the analysis. The location of three focus areas, chosen with an urban-rural gradient, is in **Fig. 1**; a national map of GmI is in **Fig. 3**; the geomorphological dataset of the three focus areas is in **Fig. 4**.

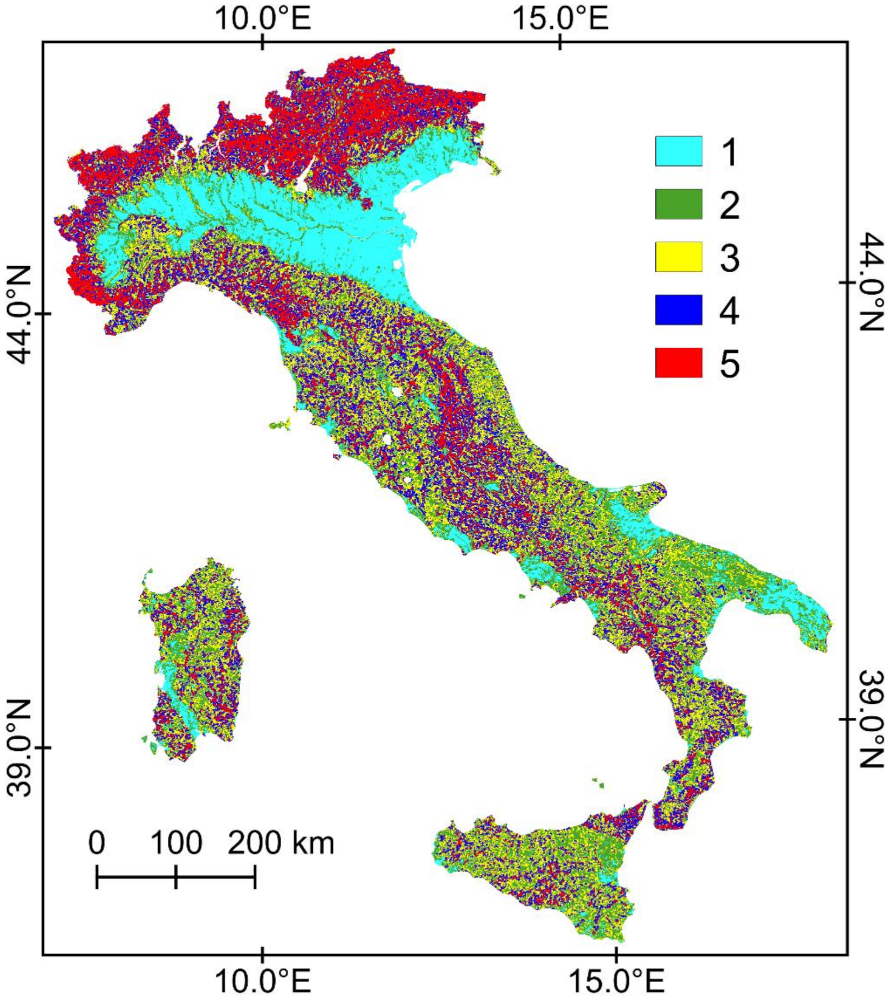

Figure 3. Land surface diversity index (GmI, throughout this work) developed following Burnelli et al. (2023). Values of GmI range from 1 (the lowest) to 5 (the highest), with a spatial resolution of 25 m.

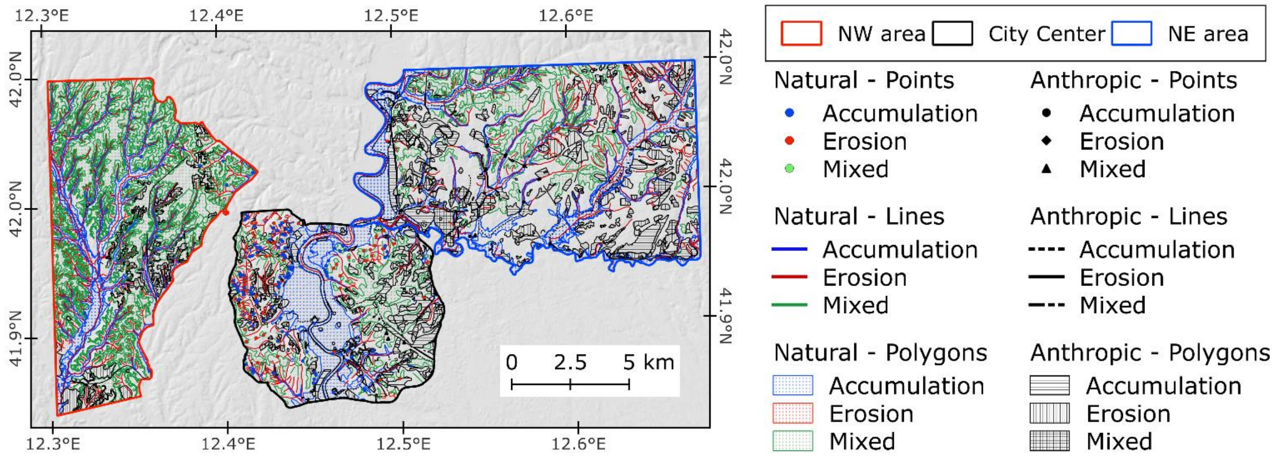

Figure 4. Geomorphological dataset of the Rome area, updated from Del Monte et al. (2016) and resulting from the ongoing geomorphological survey. The map distinguishes anthropogenic and natural features, according to morphogenetic processes corresponding to erosion, accumulation, or mixed processes. The three focus areas represent i) a natural landscape (NW area, red), ii) a modified natural landscape (NE area, blue), and iii) an anthropogenic landscape (City center area, black). They describe the distribution of natural and anthropogenic processes across the city's urban-rural gradient (see **Section 3.2**). Lithological information from Bucci et al. (2022), see Figure 1 for labels.

Figure 5. Example of landforms from the focus areas: a) modified valley in City centre area. The ancient Circus Maximum stadium was built after Murcia valley culvertion in VIth century BCE; b) landslide on marine deposits in Insugherata Natural Reserve i(NW area), the main scarp is just beneath the structural saddle, between sub-horizontal structural surfaces on both side of the hilltop; c) Man-made scarp edge (red line) highlighting the Traianum Forum depression, obtained by excavating the saddle between Capitolino and Quirinale hills in IInd century AEC. The excavation surface is the base level under the scarp. Legend of schematic section: yellow- low cohesive rocks; pink-cohesive rocks; grey- anthropogenic deposits.

Table 1. Size characteristics of natural and anthropogenic polygons of the geomorphological dataset. The analysis allowed to select the radius of the moving windows to obtain partial diversities in the calculation of GmI at the local scale.

	No.	Min area [m^2]	Max area [km^2]	Mean area [km^2]	No. poly. area > mean	No. poly. area < mean	σ [m^2]	M.W. Radius [m]
Natural polygons	616	22.77	6.81	0.17	91	525	617,924.94	215
Anthropogenic polygons	629	39.89	1.07	0.06	183	446	102,066.82	121

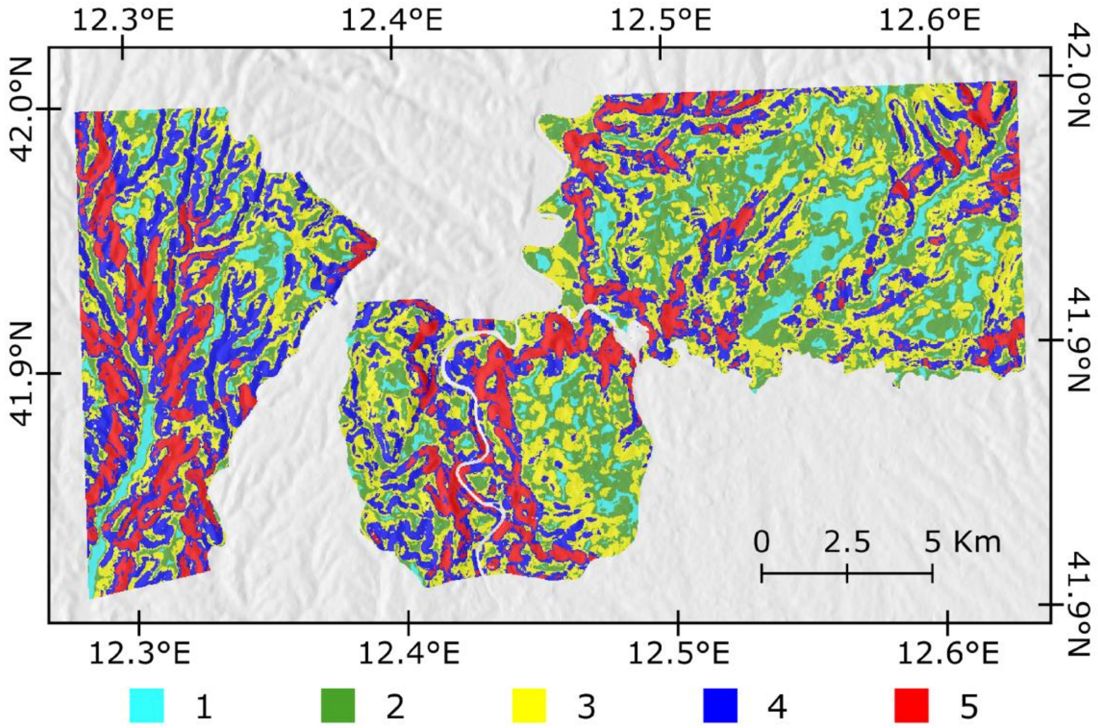

Figure 6. Land surface diversity, GmI, obtained at local scale, within the three focus area of Rome with a natural-urbanized gradient (see **Section 3.2**). The map is classified into five classes, and has spatial resolution of 25 m. **Section 4.2** describes the procedure adopted here to calculate the local GmI, modified from Burnelli et al. (2023).

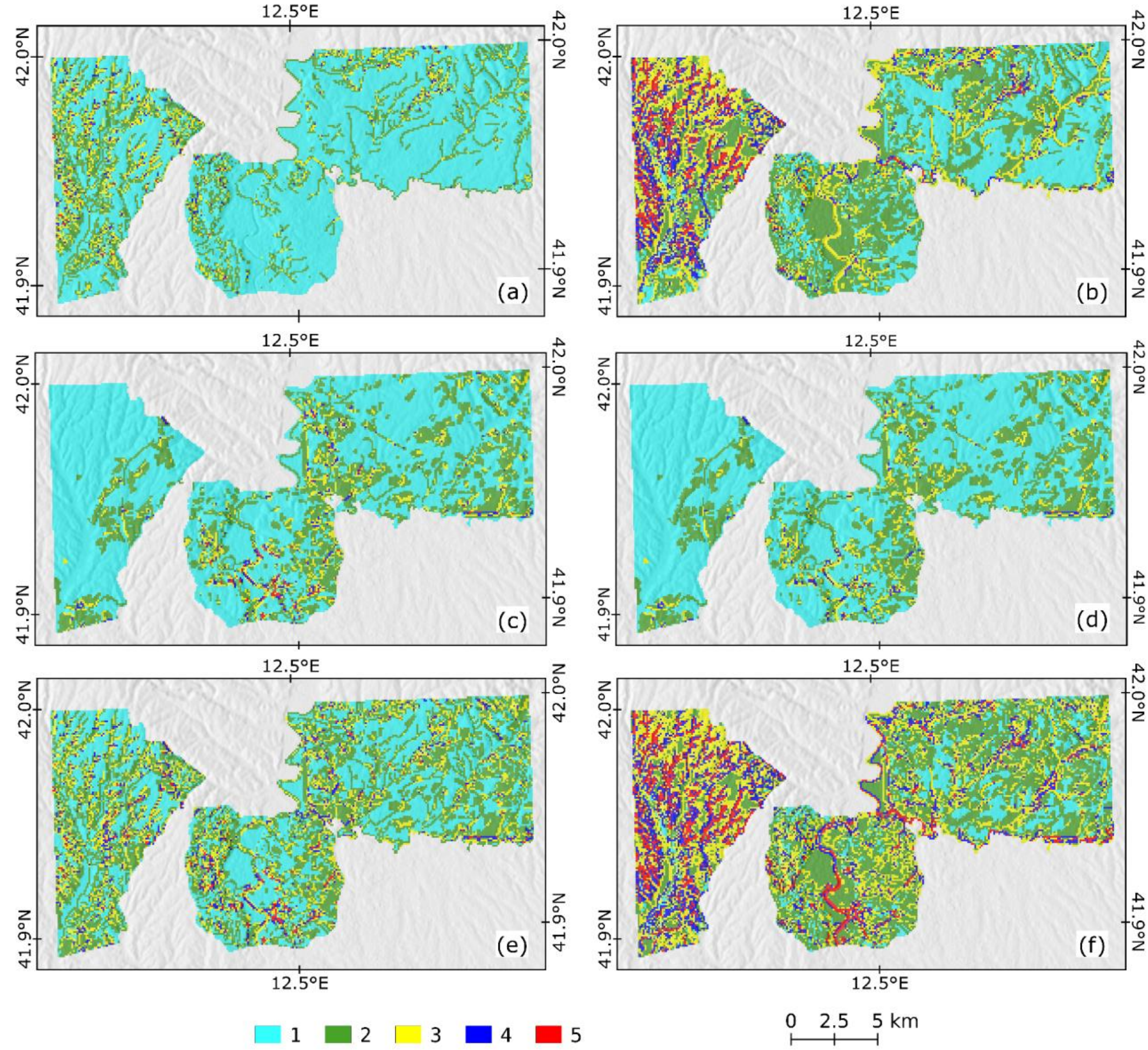

Figure 7. Maps showing the spatial distribution of the natural and anthropogenic landforms: (a) number and (b) diversity of natural features; (c) number and (d) diversity of anthropogenic features; (e) number and (f) the diversity of all of the landforms. The raster maps are classified with values ranging from 1 (the lowest) to 5 (the highest). The procedure to obtain and classify the maps is in **Section 3.3**.

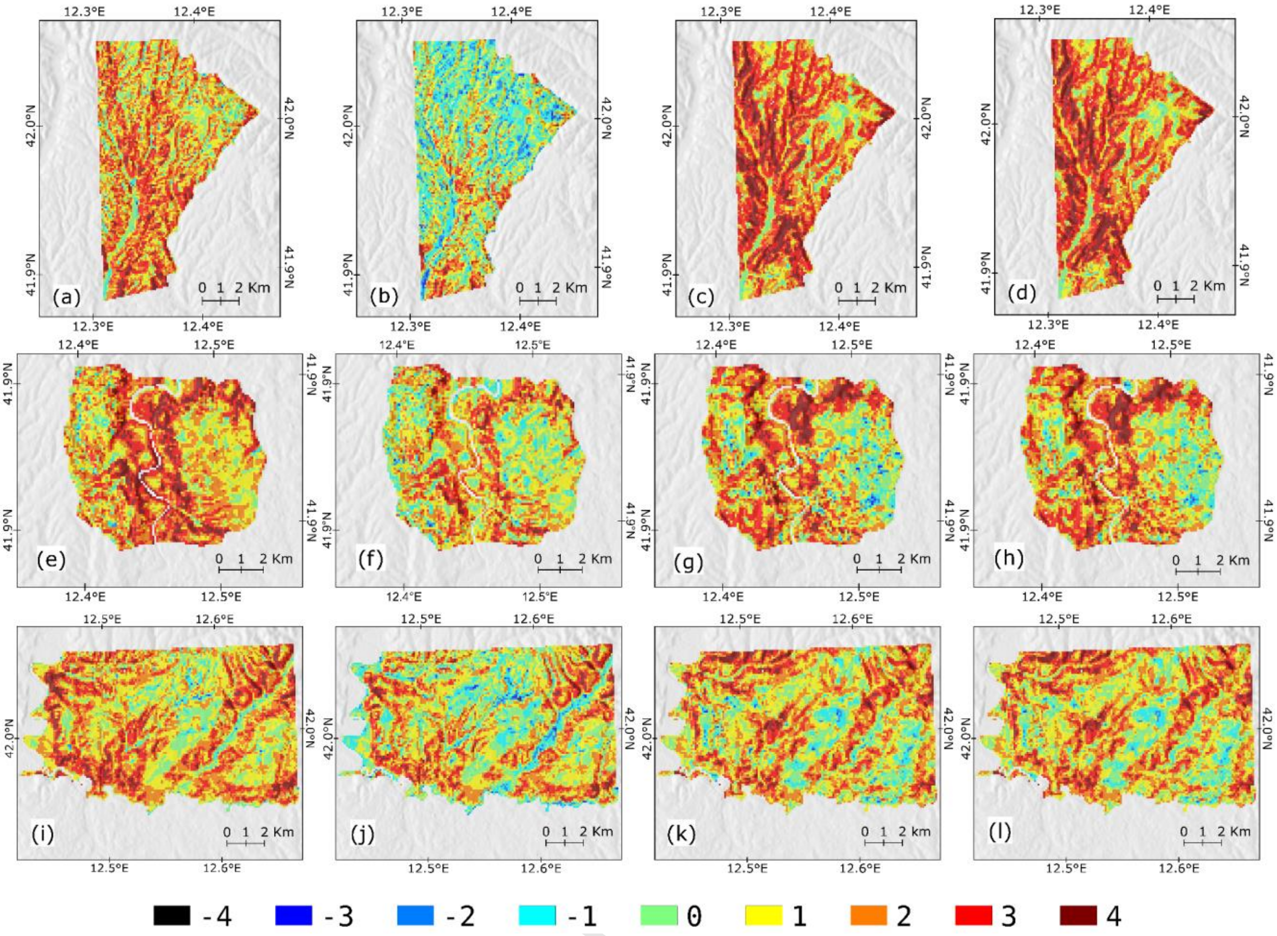

Figure 8. Raster maps showing the difference between GmI and the distribution of landforms within the three focus areas with an urban-rural gradient (see Section 3.2). Three rows describe the rural (NW, top), urban (City center, middle), and urban-rural (NE, bottom) focus areas. The columns describe the difference between the GmI and the number of natural landforms (a, e, i), the diversity of natural landforms (b, f, j), the number of anthropogenic landforms, (c, g, k), the diversity of anthropogenic landforms (d, h, l).

Table 2. Comparison between GmI values and distributions of landforms within the three focus areas. Difference represents the raster difference calculated in GIS.

	Difference	NW area (rural)	City center (urban)	NE area (urban-rural)
No. Natural	+4	5%	11%	6%
	+3	23%	22%	18%
	+2	32%	31%	29%
	+1	25%	26%	30%
	0	13%	8%	14%
	-1	3%	1%	2%
	-2	0%	0%	0%
	-3	0%	0%	0%
	-4	0%	0%	0%
Variability natural	+4	1%	3%	3%
	+3	5%	13%	12%
	+2	13%	25%	23%
	+1	24%	31%	28%
	0	29%	20%	21%
	-1	21%	6%	10%
	-2	7%	1%	2%
	-3	1%	0%	0%
	-4	0%	0%	0%
No. anthropogenic	+4	15%	8%	5%
	+3	34%	20%	15%
	+2	26%	25%	27%
	+1	16%	24%	30%
	0	8%	15%	18%
	-1	1%	5%	6%
	-2	0%	1%	1%
	-3	0%	0%	0%
	-4	0%	0%	0%
Variability anthropogenic	+4	15%	8%	5%
	+3	34%	21%	15%
	+2	26%	26%	27%
	+1	16%	25%	30%
	0	8%	15%	17%
	-1	0%	4%	5%
	-2	0%	1%	1%
	-3	0%	0%	0%
	-4	0%	0%	0%

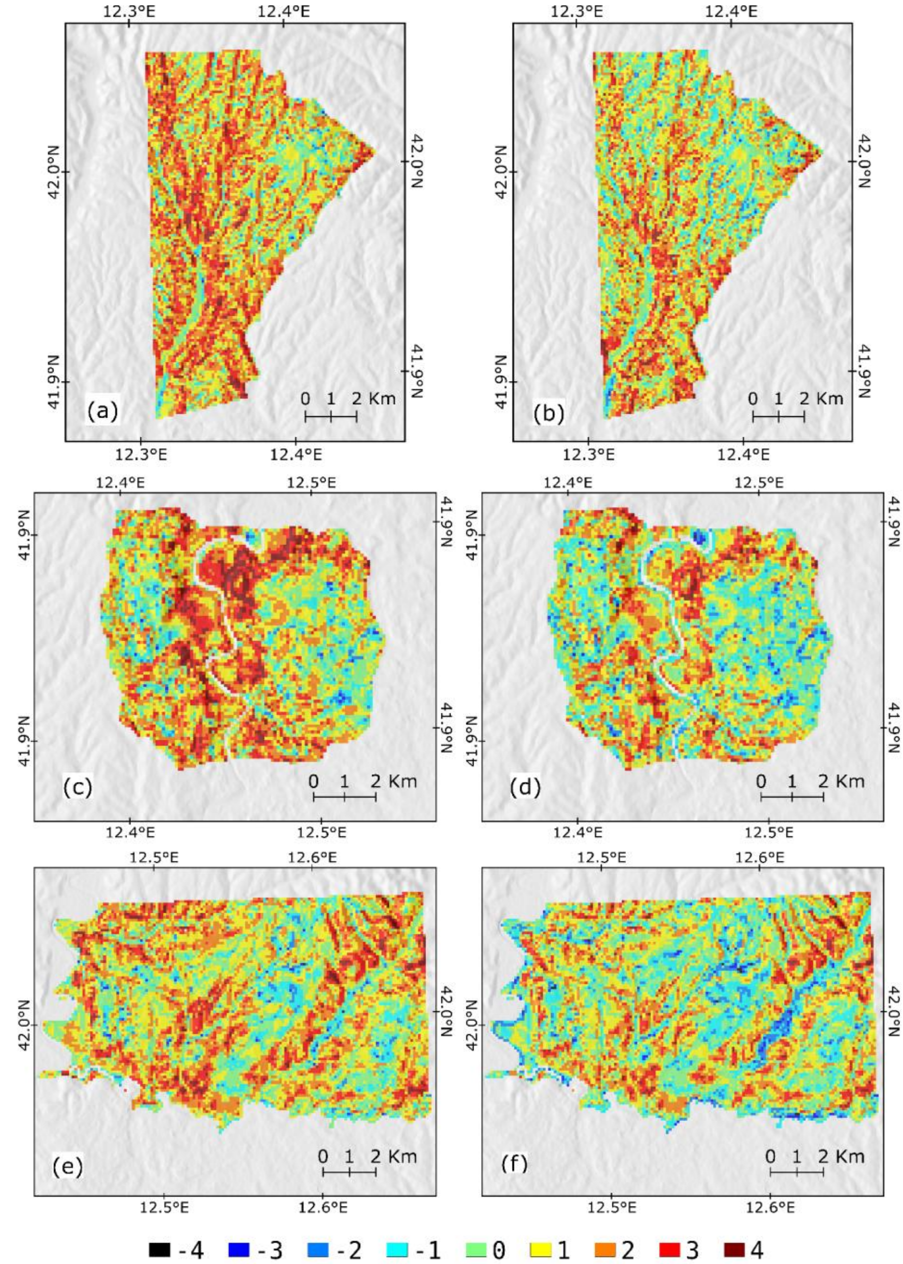

Figure 9. Maps showing the difference between GmI and the total number of the landforms (a, c, e) and the diversity of the landforms (b, d, f). The three rows of figures show focus areas with an urban-rural gradient, as in Fig. 8 (see Section 3.2)

Table 3. Comparison between the GmI and (a) the total number of the landforms and (b) the total diversity of the landforms, within the three focus areas with an urban-rural gradient (see Section 3.2). The method is described in Section 3.3 and the result is shown in Fig. 9.

	Absolute difference	**NW area (rural)**	**City center (urban)**	**NE area (urban-rural)**
(a) Total number of landforms	**+4**	**3%**	**6%**	**2%**
	+3	**18%**	**15%**	**11%**
	+2	**31%**	**25%**	**24%**
	+1	**27%**	**26%**	**30%**
	0	**16%**	**19%**	**22%**
	-1	**4%**	**8%**	**8%**
	-2	**1%**	**2%**	**2%**
	-3	**0%**	**0%**	**0%**
	-4	**0%**	**0%**	**0%**
(b) Total diversity of landforms	**+4**	**2%**	**2%**	**1%**
	+3	**11%**	**8%**	**7%**
	+2	**24%**	**19%**	**18%**
	+1	**30%**	**26%**	**26%**
	0	**23%**	**26%**	**26%**
	-1	**9%**	**15%**	**15%**
	-2	**1%**	**4%**	**5%**
	-3	**0%**	**1%**	**1%**
	-4	**0%**	**0%**	**0%**

Table 4. Values of the indicator defined in Eq. (1), summarizing the agreement between the values of GmI with respect to the map obtained as diversity of the features from geomorphological survey, and with respect to the number of features. We distinguished the three focus areas of Fig. (1). Values larger than 1/5 correspond to a prediction better than a random guess**.**

		GmI vs. diversity	**GmI vs. number**
North West	**Match**	**0.25**	**0.22**
	+/- 1	**0.67**	**0.63**
	+/- 2	**0.88**	**0.87**
City Center	**Match**	**0.24**	**0.26**
	+/- 1	**0.64**	**0.63**
	+/- 2	**0.86**	**0.86**
North East	**Match**	**0.23**	**0.24**
	+/- 1	**0.62**	**0.63**
	+/- 2	**0.88**	**0.87**

Table 5. GmI values characterizing individual natural landform types. Process type E correspond to erosion landforms, and A to

constructional landforms.

Process type	Landform type	Area [km^2]	GmI Min	GmI Max	GmI mean	GmI st. dev.
-	**Sub-horizontal structural surface**	32.69	1	5	2.75	1.11
A	**Floodplain and recent terraces**	13.02	1	5	2.75	1.10
E	**Area affected by solifluction**	0.02	2	4	3.00	1.00
E	**Surface affected by rill-interill erosion**	0.42	1	5	3.17	1.04
E	**Surface affected by concentrated washing away**	0.10	2	4	3.30	0.64
A	**Alluvial plain**	33.38	1	5	3.37	1.10
-	**Sub-structural surface**	23.29	1	5	3.39	1.06
A	**Colluvial cone**	0.03	3	4	3.67	0.47
A	**Terrace surface (fluvial)**	1.47	1	5	3.74	0.94
A	**Earth/mud flow body**	0.07	3	5	3.86	0.64
A	**Alluvial fan**	0.09	3	4	3.89	0.31
A	**Rotational slide body**	0.11	3	5	3.91	0.67
A	**Undifferentiated landslide body**	0.01	4	4	4.00	0.00
A	**Translational slide body**	0.01	4	4	4.00	0.00

Table 6. GmI values characterizing individual anthropogenic landform types. Process type E correspond to erosion landforms, A to constructional landforms, and M to mixed erosion/constructional landforms.

Process type	Landform type	Area [km^2]	GmI Min	GmI Max	GmI Mean	GMI st. dev
E	Quarry/mine	0.16	1	4	2.63	0.86
A	Filling surface in: ancient quarry	0.52	1	5	2.77	0.95
M	Surface remodeled by agricultural activity or building industry	4.41	1	5	2.77	1.26
A	Filling surface in: ancient valley	9	1	5	2.84	1.04
A	Reservoir	0.15	1	5	2.87	0.96
A	Ridge created for: motorway / railway / dumping	2.07	1	5	2.90	1.00
A	Embankment/infill	7.79	1	5	2.90	1.09
E	Abandoned quarry/mine	1.90	1	5	3.33	1.06
E	Trench	0.06	3	4	3.33	0.47
A	Filling surface in: generic anthropic depression	0.14	1	5	3.36	0.97
E	Excavation surface	2.29	1	5	3.40	1.22
M	Terraced slope by: building industry	8.94	1	5	3.48	1.05
A	Landfill area/dump	0.87	2	5	3.76	1.03
M	Terraced slope by: agricultural activity	0.19	2	5	3.84	1.04
A	Artificial hill	0.13	2	5	3.85	0.86

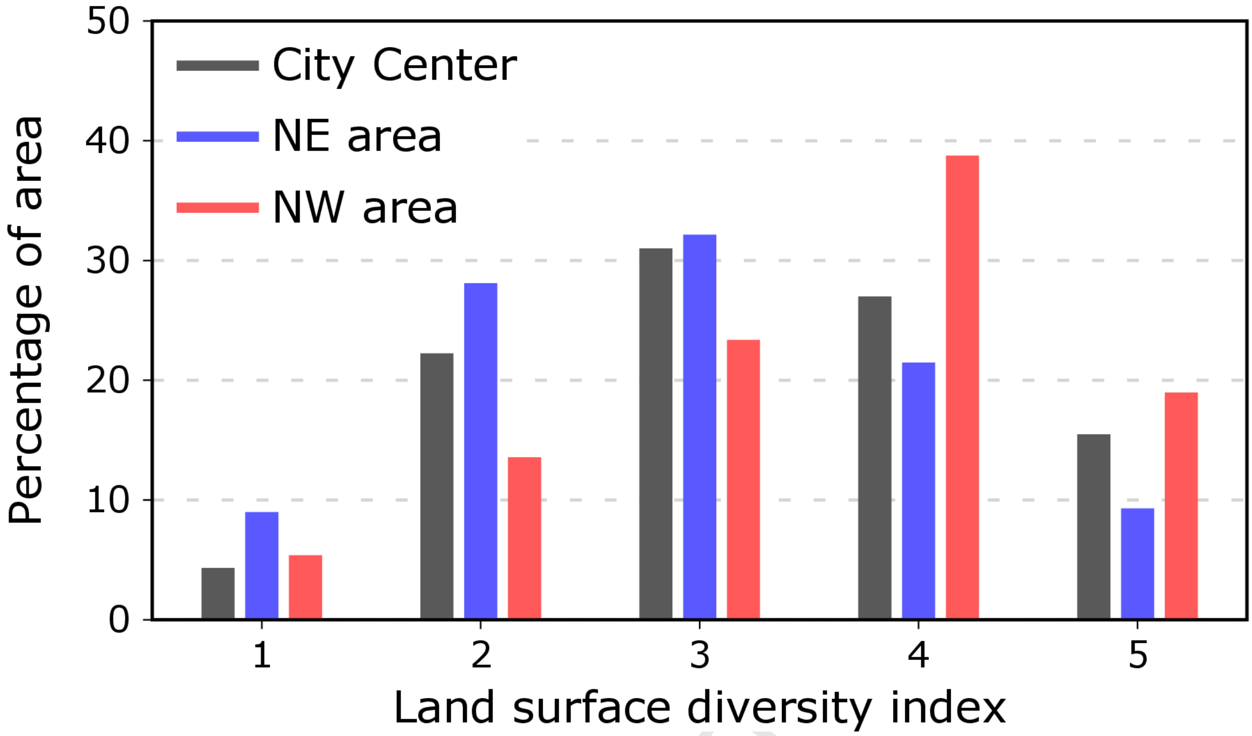

Figure 10. Percentage of GmI classes in the three focus areas. Values represent aggregated natural and anthropogenic landforms.

Table 7. Correspondence between the GMI and the number and diversity of natural, anthropogenic and total landforms in each focus area. Abbreviation NAT denotes natural landforms, ANT anthropogenic landforms.

		NW area (rural) %	City center (urban)%	NE area (urban-rural)%
Good correspondence (values -2 to +2)	Number NAT	73	67	76
	Diversity NAT	94	84	85
	Number ANT	51	70	80
	Diversity ANT	50	71	80
	Total number of landforms	79	80	87
	Total diversity of landforms	87	90	91
Overestimation (values ≥ 3)	Number NAT	27	33	24
	Diversity NAT	5	16	15
	Number .ANT	49	30	20
	Diversity ANT	50	29	20
	Total number of landforms	21	20	13
	Total diversity of landforms	13	9	8
Underestimation (value ≤ -3)	Number NAT	0	0	0
	Diversity NAT	1	0	0
	Number ANT	0	0	0
	Diversity ANT	0	0	0
	Total number of landforms	0	0	0
	Total diversity of landforms	0	1	1

Declaration of interests

☒The authors declare that they have no known competing financial interests or personal relationships that could have appeared to influence the work reported in this paper.

☐The authors declare the following financial interests/personal relationships which may be considered as potential competing interests:

Does anthropogenic morphogenesis contribute to geomorphodiversity in urban environments?

Martina Burnelli[1,2], Alessia Pica[3]*, Maurizio Del Monte[3], Michele Delchiaro[3], Laura Melelli[1], Francesca Reame[3], Francesca Vergari[3], Massimiliano Alvioli[2]

[1] Department of Physics and Geology, University of Perugia, Piazza Università 1, 06123, Perugia, Italy

[2] Istituto di Ricerca per la Protezione Idrogeologica, Consiglio Nazionale delle Ricerche, via Madonna Alta 126, I-06128, Perugia, Italy

[3] Sapienza University of Rome, Earth Sciences p.zzle A. Moro 5, 00185 Rome, Italy

*Correspondence: alessia.pica@uniroma1.it

Highlights

- Anthropogenic morphogenesis modifies natural landscape in urban environments
- Locally scaled-down land surface diversity index matches real-world geomorphology
- Anthropogenic landforms contribute to geomorphodiversity as much as natural ones

Table 1. Size characteristics of natural and anthropogenic polygons of the geomorphological dataset. The analysis allowed to select the radius of the moving windows to obtain partial diversities in the calculation of GmI at the local scale.

	No.	Min area [m^2]	Max area [km^2]	Mean area [km^2]	No. poly. area > mean	No. poly. area < mean	σ [m^2]	M.W. Radius [m]
Natural polygons	616	22.77	6.81	0.17	91	525	617,924.94	215
Anthropogenic polygons	629	39.89	1.07	0.06	183	446	102,066.82	121

Table 2. Comparison between GmI values and distributions of landforms within the three focus areas. Difference represents the raster difference calculated in GIS.

	Difference	**NW area (rural)**	**City center (urban)**	**NE area (urban-rural)**
No. Natural	**+4**	**5%**	**11%**	**6%**
	+3	**23%**	**22%**	**18%**
	+2	**32%**	**31%**	**29%**
	+1	**25%**	**26%**	**30%**
	0	**13%**	**8%**	**14%**
	-1	**3%**	**1%**	**2%**
	-2	**0%**	**0%**	**0%**
	-3	**0%**	**0%**	**0%**
	-4	**0%**	**0%**	**0%**
Variability natural	**+4**	**1%**	**3%**	**3%**
	+3	**5%**	**13%**	**12%**
	+2	**13%**	**25%**	**23%**
	+1	**24%**	**31%**	**28%**
	0	**29%**	**20%**	**21%**
	-1	**21%**	**6%**	**10%**
	-2	**7%**	**1%**	**2%**
	-3	**1%**	**0%**	**0%**
	-4	**0%**	**0%**	**0%**
No. anthropogenic	**+4**	**15%**	**8%**	**5%**
	+3	**34%**	**20%**	**15%**
	+2	**26%**	**25%**	**27%**
	+1	**16%**	**24%**	**30%**
	0	**8%**	**15%**	**18%**

	-1	**1%**	**5%**	**6%**
	-2	**0%**	**1%**	**1%**
	-3	**0%**	**0%**	**0%**
	-4	**0%**	**0%**	**0%**
Variability anthropogenic	**+4**	**15%**	**8%**	**5%**
	+3	**34%**	**21%**	**15%**
	+2	**26%**	**26%**	**27%**
	+1	**16%**	**25%**	**30%**
	0	**8%**	**15%**	**17%**
	-1	**0%**	**4%**	**5%**
	-2	**0%**	**1%**	**1%**
	-3	**0%**	**0%**	**0%**
	-4	**0%**	**0%**	**0%**

Table 3. Comparison between the GmI and (a) the total number of the landforms and (b) the total diversity of the landforms, within the three focus areas with an urban-rural gradient (see Section 3.2). The method is described in Section 3.3 and the result is shown in Fig. 9.

	Absolute difference	**NW area (rural)**	**City center (urban)**	**NE area (urban-rural)**
(a) Total number of landforms	**+4**	**3%**	**6%**	**2%**
	+3	**18%**	**15%**	**11%**
	+2	**31%**	**25%**	**24%**
	+1	**27%**	**26%**	**30%**
	0	**16%**	**19%**	**22%**
	-1	**4%**	**8%**	**8%**
	-2	**1%**	**2%**	**2%**
	-3	**0%**	**0%**	**0%**
	-4	**0%**	**0%**	**0%**
(b) Total diversity of landforms	**+4**	**2%**	**2%**	**1%**
	+3	**11%**	**8%**	**7%**
	+2	**24%**	**19%**	**18%**
	+1	**30%**	**26%**	**26%**
	0	**23%**	**26%**	**26%**
	-1	**9%**	**15%**	**15%**
	-2	**1%**	**4%**	**5%**
	-3	**0%**	**1%**	**1%**
	-4	**0%**	**0%**	**0%**

Table 4. Values of the indicator defined in Eq. (1), summarizing the agreement between the values of GmI with respect to the map obtained as diversity of the features from geomorphological survey, and with respect to the number of features. We distinguished the three focus areas of Fig. (1). Values larger than 1/5 correspond to a prediction better than a random guess.

		GmI vs. diversity	GmI vs. number
North West	Match	0.25	0.22
	+/- 1	0.67	0.63
	+/- 2	0.88	0.87
City Center	Match	0.24	0.26
	+/- 1	0.64	0.63
	+/- 2	0.86	0.86
North East	Match	0.23	0.24
	+/- 1	0.62	0.63
	+/- 2	0.88	0.87

Table 5. GmI values characterizing individual natural landform types. Process type E correspond to erosion landforms, and A to constructional landforms.

Process type	Landform type	Area [km^2]	GmI Min	GmI Max	GmI mean	GmI st. dev.
-	Sub-horizontal structural surface	32.69	1	5	2.75	1.11
A	Floodplain and recent terraces	13.02	1	5	2.75	1.10
E	Area affected by solifluction	0.02	2	4	3.00	1.00
E	Surface affected by rill-interill erosion	0.42	1	5	3.17	1.04
E	Surface affected by concentrated washing away	0.10	2	4	3.30	0.64
A	Alluvial plain	33.38	1	5	3.37	1.10
-	Sub-structural surface	23.29	1	5	3.39	1.06
A	Colluvial cone	0.03	3	4	3.67	0.47

A	Terrace surface (fluvial)	1.47	1	5	3.74	0.94
A	Earth/mud flow body	0.07	3	5	3.86	0.64
A	Alluvial fan	0.09	3	4	3.89	0.31
A	Rotational slide body	0.11	3	5	3.91	0.67
A	Undifferentiated landslide body	0.01	4	4	4.00	0.00
A	Translational slide body	0.01	4	4	4.00	0.00

Table 6. GmI values characterizing individual anthropogenic landform types. Process type E correspond to erosion landforms, A to constructional landforms, and M to mixed erosion/constructional landforms.

Process type	Landform type	Area [km^2]	GmI Min	GmI Max	GmI Mean	GMI st. dev
E	Quarry/mine	0.16	1	4	2.63	0.86
A	Filling surface in: ancient quarry	0.52	1	5	2.77	0.95
M	Surface remodeled by agricultural activity or building industry	4.41	1	5	2.77	1.26
A	Filling surface in: ancient valley	9	1	5	2.84	1.04
A	Reservoir	0.15	1	5	2.87	0.96
A	Ridge created for: motorway / railway / dumping	2.07	1	5	2.90	1.00
A	Embankment/infill	7.79	1	5	2.90	1.09
E	Abandoned quarry/mine	1.90	1	5	3.33	1.06
E	Trench	0.06	3	4	3.33	0.47
A	Filling surface in: generic anthropic depression	0.14	1	5	3.36	0.97
E	Excavation surface	2.29	1	5	3.40	1.22
M	Terraced slope by: building industry	8.94	1	5	3.48	1.05
A	Landfill area/dump	0.87	2	5	3.76	1.03
M	Terraced slope by: agricultural activity	0.19	2	5	3.84	1.04
A	Artificial hill	0.13	2	5	3.85	0.86